Cell Reports Medicine, Volume *5*

Supplemental information

Targeting the HSP47-collagen axis inhibits brain metastasis by reversing M2 microglial polarization and restoring anti-tumor immunity

Li Wang, Cuiying Li, Hongchao Zhan, Shangbiao Li, Kunlin Zeng, Chang Xu, Yulong Zou, Yuxin Xie, Ziling Zhan, Shengqi Yin, Yu Zeng, Xiaoxia Chen, Guangzhao Lv, Zelong Han, Dexiang Zhou, Dong Zhou, Yong Yang, and Aidong Zhou

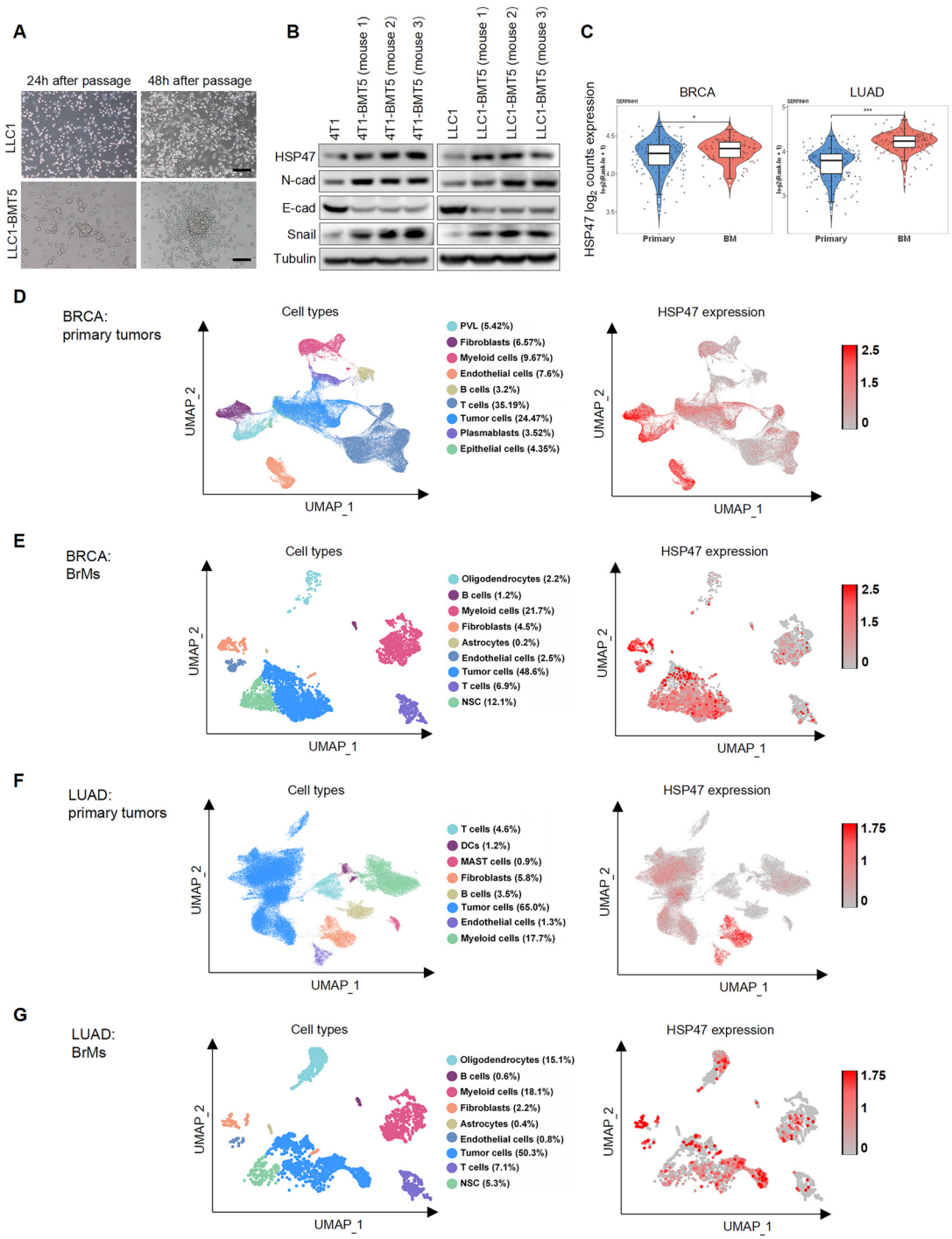

Figure S1. HSP47 is upregulated in brain metastases. Related to Figure 1.

(A) Bright-field microscope images showing the morphological changes of LLC-BMT5 cells in contrast to the parental cells. Representative images were shown. Scale bars, 100 μm.

(B) Cell lysates of 4T1-BMT5 and LLC1-BMT5 cells derived from different mice were analyzed by immunoblotting using the indicated antibodies.

(C) Violin plots showing the mRNA levels of *SERPINH1* in brain metastases from breast cancer (n=97) and lung cancer (n=144) compared with the primary tumors, respectively. The public datasets used are the same as in Figure 1A. *$p < 0.05$, ***$p < 0.001$.

(D-G) ScRNA-seq showing the expression of HSP47 in different cell types in breast cancer BrMs (n=3) (GSE234832) with corresponding primary tumors (n=26) (GSE176078), and in lung cancer BrMs (n=2) (GSE234832) with corresponding primary tumors (n=42) (GSE148071).

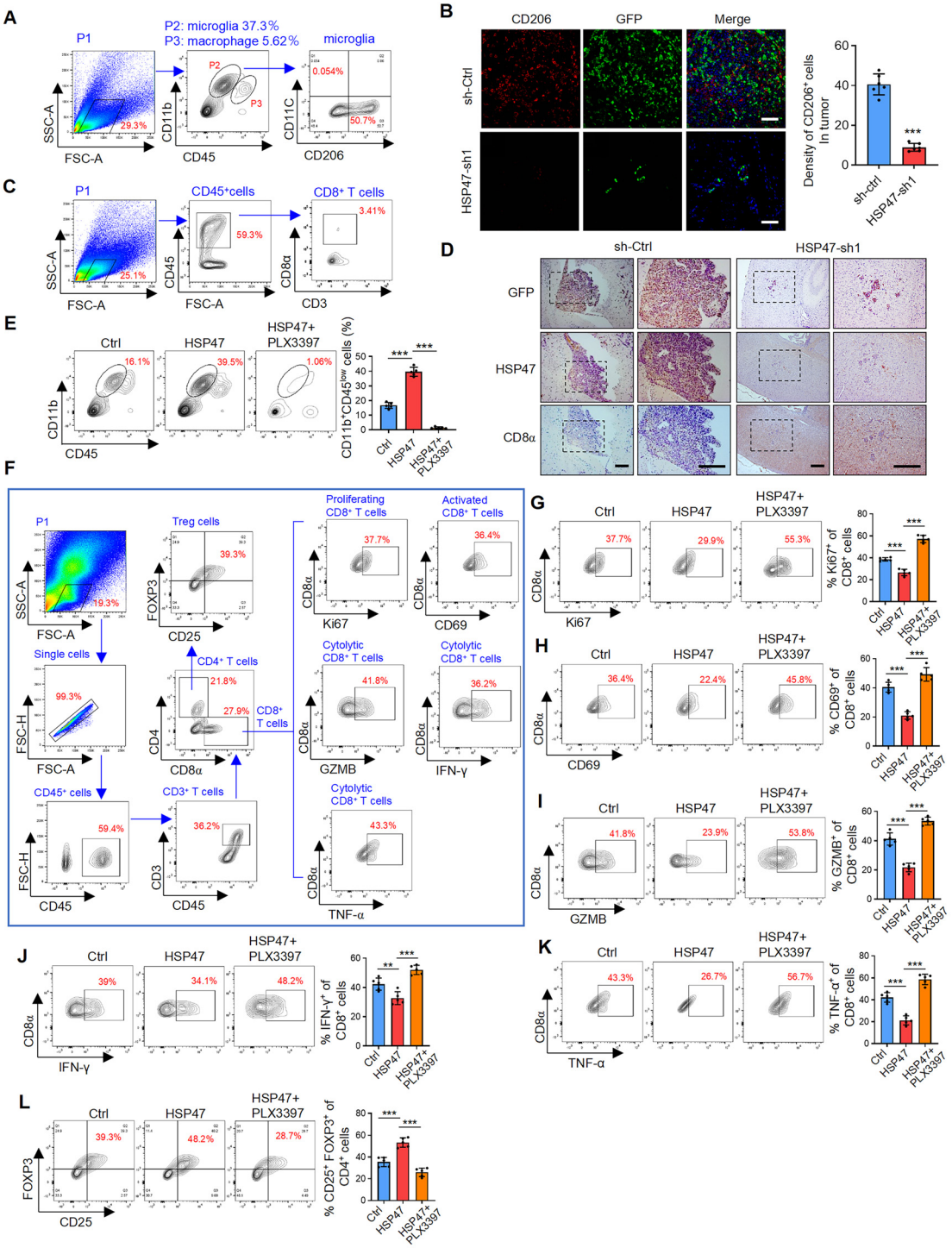

Figure S2. HSP47 promotes M2 microglial polarization and immunosuppression. Related to Figure 3.

(A) Gating strategy for profiling microglia and macrophages by FACS in Figure 3A.

(B) 4T1-BMT5 cells expressing control shRNA or HSP47 shRNA were transfected with the GFP gene and then intracardially injected into mice. The mouse BrMs derived from 4T1-BMT5 cells were double stained with the antibodies against GFP and CD206. Representative images were shown. Scale bars, 100 μm. The density of $CD206^+$ cells in each microscope field was counted (n=6 randomly selected fields, mean ± S.E.M, Student's *t*-tests). ***p < 0.001.

(C) Gating strategy for profiling $CD8^+$ T cells by FACS in Figure 3C.
(D) Consecutive mouse brain metastatic tissues derived from 4T1-BMT5 cells were stained with antibodies against GFP, HSP47 and CD8α. Scale bars, 200 μm.
(E) Representative FACS plots and quantification of $CD11b^+CD45^{low}$ cells in mouse BrMs after treatment by PLX3397 (mean ± SEM, n=5 independent experiments, Student's *t*-tests). ***p < 0.001.
(F) Gating strategy for profiling $CD8^+$ and $CD4^+$ T cell subpopulations by FACS in Figures 3J-3M.
(G-L) Representative FACS plots and quantification of $Ki67^+$, $CD69^+$, $GZMB^+$, IFN-γ^+, TNF-α^+ of $CD8^+$ T cells and $CD25^+FOXP3^+CD4^+$ Tregs in Figures 3J-M (mean ± SEM, n=5 independent experiments, Student's *t*-tests). **p < 0.01, ***p < 0.001.

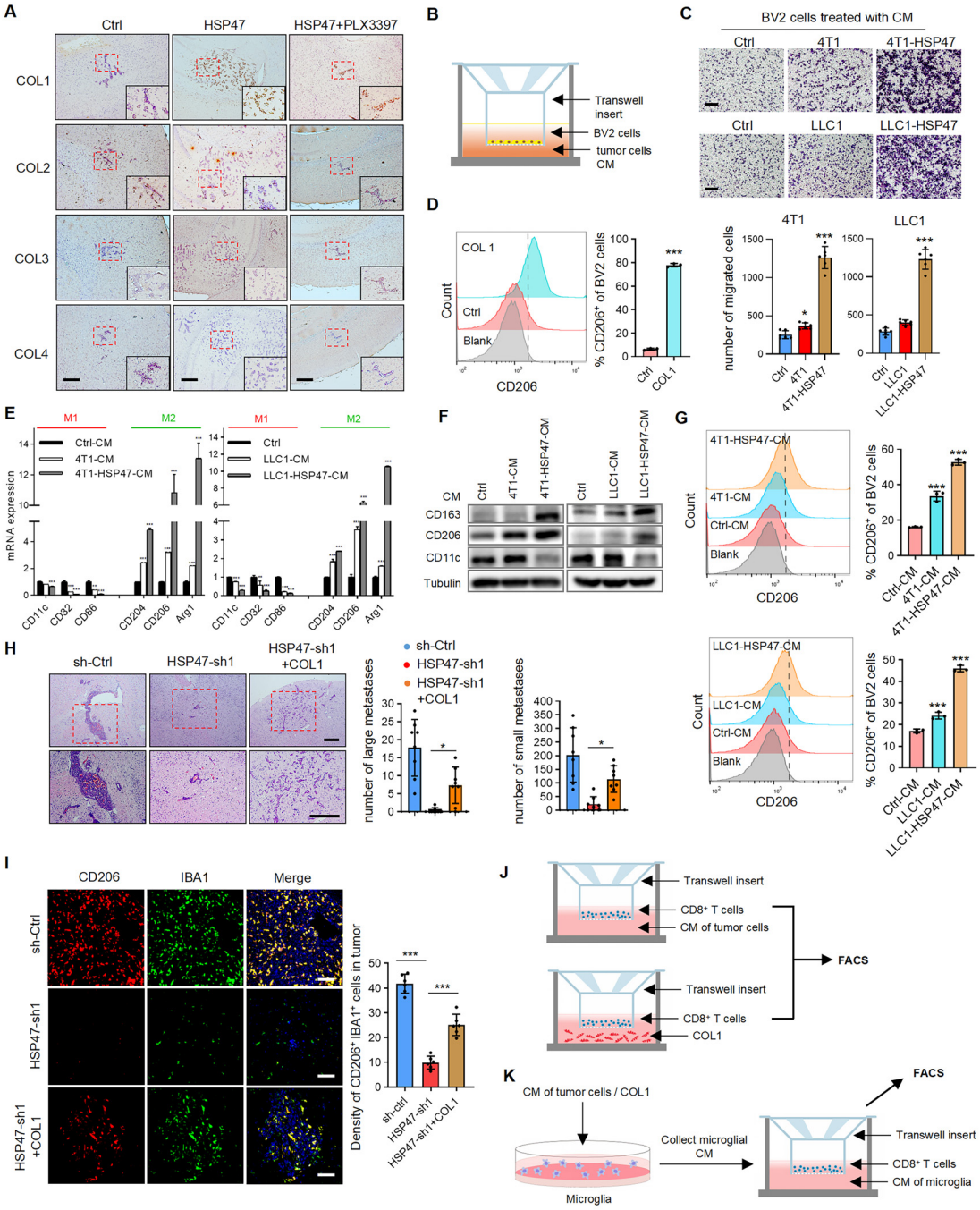

Figure S3. COL1 mediates HSP47-induced microglia recruitment and M2 polarization. Related to Figure 4.

(A) Consecutive mouse BrM tissues were analyzed by IHC staining using the antibodies against COL1-4. Scale bars, 200 μm. Insets: high-magnification images corresponding to the areas marked by red dotted lines.

(B) Scheme shows the experiment procedure of microglia recruitment by the CM of cancer cells.

(C) BV2 cells were cultured in the CM of 4T1 or LLC1 cells expressing HSP47, and cells migrated onto the lower surface of the transwell chamber were stained by crystal violet. Representative images were shown. Scale bars, 100 μm. Data were presented as mean ± SEM of n=6 randomly selected microscope fields of two independent experiments, Student's *t*-tests, ***p < 0.001.

(D) BV2 cells were treated with COL1 and the expression of CD206 was analyzed by FACS. FACS data were statistically analyzed (mean±SD, n=3 independent experiments, Student's *t*-tests), ***p < 0.001.
(E) BV2 cells were cultured in the CM of 4T1 or LLC1 cells expressing HSP47, and the mRNA levels of indicated genes were analyzed by qRT-PCR. *GAPDH* was used as an internal control (mean ± SEM, n=3 independent experiments, two-tailed Student's t-test). **p < 0.01, ***p < 0.001.
(F) BV2 cells were treated as in (E), and cell lysates were analyzed by immunoblotting using the indicated antibodies.
(G) BV2 cells were treated as in (E) and the expression of CD206 was analyzed by FACS (mean ± SEM, n=3 independent experiments, Student's *t*-tests), ***p < 0.001.
(H) H&E staining of BrMs in mice. Representative images were shown. Scale bars, 200 μm. Insets: high-magnification images corresponding to the areas marked by red dotted lines. The BrMs were quantified. Large metastases are >300 μm on the longest axis (mean ± SD, n=8 mice, two-sided Mann-Whitney test). *p < 0.05.
(I) Mouse BrM tissues derived from 4T1-BMT5 cells were double-stained with IBA1 and CD206. Representative images were shown. Scale bars, 100 μm. The density of IBA1 and CD206 positive cells was counted (mean ± SEM, n=6 randomly selected microscope fields, Student's *t*-tests), ***p < 0.001.
(J) Scheme shows the experiment procedure of $CD8^+$ T cells recruitment by COL1 (4mg/mL) or the CM of tumor cells overexpressing HSP47.
(K) Scheme shows the experiment procedure of $CD8^+$ T cells recruitment by the CM of microglia. Microglia were treated with 4 mg/mL COL1 or the CM of tumor cells overexpressing HSP47, and then the culture medium was replaced with fresh medium. $CD8^+$ T cells in the upper chamber were cultured with the CM of microglia, and cells migrated onto lower surface of the transwell chamber were counted by FACS.

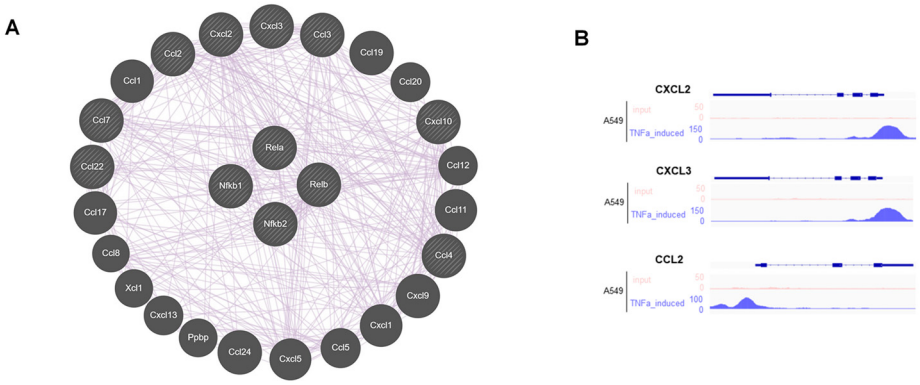

Figure S4. COL1 promotes microglial polarization through the β-Integrin/NF-κB signaling. Related to Figure 5.

(A) GeneMANIA (genemania.org) protein-protein interaction network of the genes regulated by COL1 in BV2 cells.

(B) ChIP-seq data analysis demonstrated that NF-κB binds to the promoter regions of CXCL2, CXCL3, CCL2 genes in A549 cells (GSM847875, GSM847876 and GSM847877).

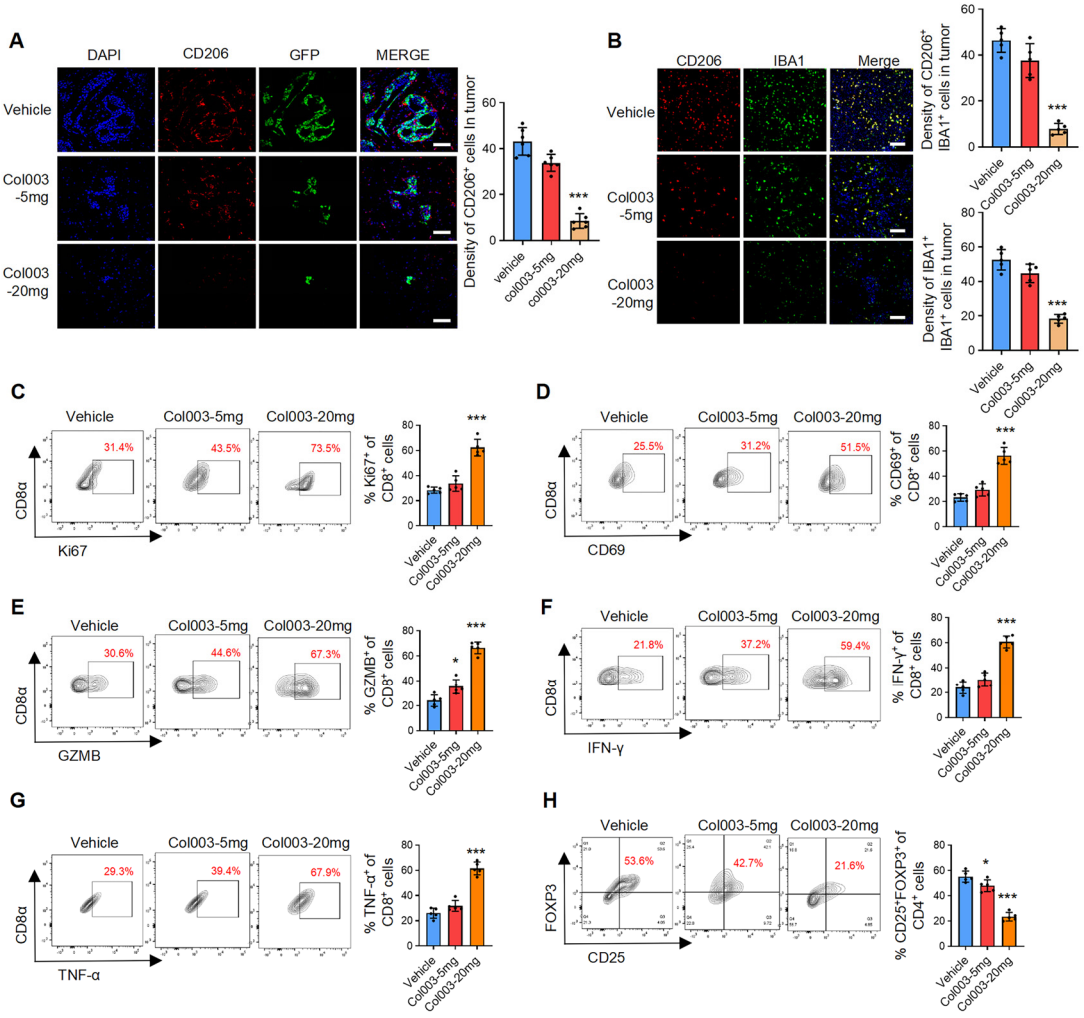

Figure S5. Targeting HSP47-mediated COL1 biosynthesis inhibits brain metastasis. Related to Figure 6.

(A) 4T1-BMT5 cells were engineered to express GFP and then intracardially injected into mice. Mouse BrM tissues were double-stained with CD206 and GFP. Representative images were shown. Scale bars, 100 μm. The density of CD206 positive cells was counted (mean ± SEM, n=6 randomly selected microscope fields, Student's *t*-tests), ***p < 0.001.

(B) Mouse BrM tissues derived from 4T1-BMT5 cells were double-stained with CD206 and IBA1. Representative images were shown. Scale bars, 100 μm. The density of CD206 and IBA1 positive cells was counted (mean ± SEM, n=6 randomly selected microscope fields, Student's *t*-tests), ***p < 0.001.

(C-H) Representative FACS plots and quantification of percentages of Ki-67$^+$, CD69$^+$, GZMB$^+$, IFN-γ$^+$, TNF-α$^+$ CD8$^+$ T cells and CD25$^+$FOXP3$^+$CD4$^+$ Tregs in Figures 6I- 6L (mean ± SEM, n=5 independent experiments, Student's *t*-tests), **p < 0.01, ***p < 0.001.

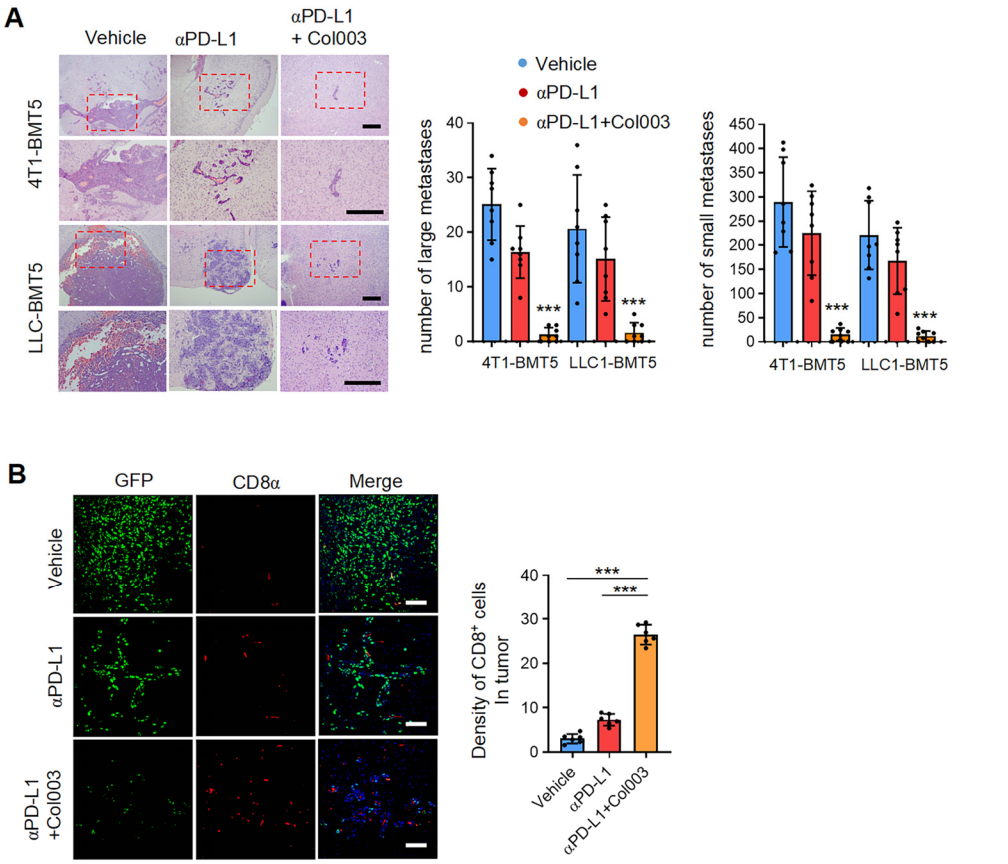

Figure S6. Col003 augments the therapeutic efficacy of anti-PD-L1 antibody in brain metastases. Related to Figure 7.

(A) The brain metastases-bearing mice derived from 4T1-BMT5 and LLC1-BMT5 cells were treated with anti-PD-L1 antibody alone or anti-PD-L1 antibody plus Col003. The BrM tissues were stained by H&E. Representative images were shown. Scale bars, 200 μm. The number of BrMs were quantified. Large metastases are >300 μm on the longest axis (n=8 mice, two-sided Mann-Whitney test). ***p < 0.001.

(B) 4T1-BMT5 cells were engineered to express GFP and then intracardially injected into mice. The brain metastatic tissues were double-stained with CD8α and GFP. Representative images were shown. Scale bars, 100 μm. ***p < 0.001.

Table S1. Patient characteristics. Related to STAR Methods.

ID	disease	gender	age
P837605	LUAD BrM	M	60
P357220	LUAD BrM	M	59
P355113	LUAD BrM	F	66
P827382	LUAD BrM	M	50
P229500	LUAD BrM	M	68
P890850	LUAD BrM	F	51
P546874	LUAD BrM	F	52
P668022	LUAD BrM	M	51
P687444	LUAD BrM	M	65
P619045	LUAD BrM	F	58
P626454	LUAD BrM	M	35
P621745	LUAD BrM	M	58
P629765	LUAD BrM	F	55
P638733	LUAD BrM	F	60
P894798	LUAD BrM	F	36
P726108	LUAD BrM	M	60
P605370	LUAD BrM	M	49
P633770	LUAD BrM	M	57
P635249	LUAD BrM	M	48
P890866	LUAD BrM	M	59
P573499	LUAD BrM	M	64
P650646	LUAD BrM	M	79
P691305	LUAD BrM	M	73
P718836	LUAD BrM	M	67
P747731	LUAD BrM	F	61
P720222	LUAD BrM	M	71
P288819	BRCA BrM	F	44
P434561	BRCA BrM	F	53
P205316	BRCA BrM	F	21
P663583	BRCA BrM	F	35
P771293	BRCA BrM	F	42
P924213	BRCA BrM	F	49
P827314	BRCA BrM	F	57
P835390	BRCA BrM	F	69
P772335	BRCA BrM	F	66
P412337	BRCA BrM	F	59
P991250	BRCA BrM	F	77
P252839	BRCA BrM	F	64

Table S2. List of oligos used in the study. Related to STAR Methods.

gene	sequence
For qPCR	
m-SERPINH1-F	GCCGAGGTGAAGAAACCCC
m-SERPINH1-R	CATCGCCTGATATAGGCTGAAG
m-S100A6-F	CCAGACTGCGACACATTCCA
m-S100A6-R	TGGGCTAGAAGAAGCGCAC
m-S100A11-F	GCTGCCTTCACAAAGAACCAG
m-S100A11-R	CACGCTATAGCTAAGCCACCA
m-S100A13-F	AACTGCCTCATTTGCTCAAGG
m-S100A13-R	AGTCTCCAGTATTCACTGAACCT
m-LAMA5-F	GCTGGCGGAGATCCCAATC
m-LAMA5-R	GTGTGACGTTGACCTCATTGT
m-ANXA6-F	CACAGGGTGCCATGTACCG
m-ANXA6-R	TCCTGATTTGCGTCAAACTCTG
m-HCFC1-F	CGGCAACGAGGGGATAGTG
m-HCFC1-R	TAGGCGAGTACCATCACACAC
m-CTSA-F	CGTGTGATAGCGAAGACCCA
m-CTSA-R	GGTTCCGGGCATGTCTTGG
m-CSTB-F	CGACTACTGCTGCCAAGATGA
m-CSTB-R	GCTGGGACTTCACCTGGTCG
m-CTSD-F	TACTCCATGCAGTCATCGCC
m-CTSD-R	CGCCATAGTACTGGGCATCC
m-PLXNB2-F	TCTGTCTGTACCAGTACCTCAAG
m-PLXNB2-R	CGCATACTCAACATCGTCCC
m-LTBP3-F	GAACCTCCAGGGCTCCTATGT
m-LTBP3-R	GTAGCACTCCTTCTTGTGGTG
m-AGRN-F	GCGGTACTTGAAAGGCAAAGA
m-AGRN-R	CTCCAAAGCCACCAATTACCA
m-CBLN1-F	AGACAGACCATCCAGGTGAGC
m-CBLN1-R	GCTTGAGGTATGCTCGGTCG
m-PLOD1-F	TTCGTCGTCCGCTATAAGCC
m-PLOD1-R	GCAACCTCCGCCCTCATAAT
m-CD204-F	GCACAATCTGTGATGATCGCT
m-CD204-R	CCCAGCATCTTCTGAATGTGAA
m-CD206-F	GTTCACCTGGAGTGATGGTTCTC
m-CD206-R	AGGACATGCCAGGGTCACCTTT
m-CD32-F	AATCCTGCCGTTCCTACTGATC
m-CD32-R	GTGTCACCGTGTCTTCCTTGAG
m-CD11C-F	CTGGATAGCCTTTCTTCTGCTG

m-CD11C-R	GCACACTGTGTCCGAACTCA
m-CD86-F	TGTTTCCGTGGAGACGCAAG
m-CD86-R	TTGAGCCTTTGTAAATGGGCA
m-Arg1-F	CTCCAAGCCAAAGTCCTTAGAG
m-Arg1-R	AGGAGCTGTCATTAGGGACATC
m-Ccl2-F	TTAAAAACCTGGATCGGAACCAA
m-Ccl2-R	GCATTAGCTTCAGATTTACGGGT
m-Ccl3-F	TTCTCTGTACCATGACACTCTGC
m-Ccl3-R	CGTGGAATCTTCCGGCTGTAG
m-Ccl4-F	TTCCTGCTGTTTCTCTTACACCT
m-Ccl4-R	CTGTCTGCCTCTTTTGGTCAG
m-Ccl7-F	CCCTGGGAAGCTGTTATCTTCAA
m-Ccl7-R	CTCGACCCACTTCTGATGGG
m-Ccl9-F	CCCTCTCCTTCCTCATTCTTACA
m-Ccl9-R	AGTCTTGAAAGCCCATGTGAAA
m-Ccl22-F	CCAAAAGATACTGAACAAAGGCA
m-Ccl22-R	CTTGCGGCAGGATTTTGAGG
m-Cxcl2-F	CCAAAAGATACTGAACAAAGGCA
m-Cxcl2-R	CGAGGCACATCAGGTACGA
m-Cxcl3-F	CCAGACAGAAGTCATAGCCAC
m-Cxcl3-R	CTTCATCATGGTGAGGGGCTT
m-Cxcl10-F	CCAAGTGCTGCCGTCATTTTC
m-Cxcl10-R	GGCTCGCAGGGATGATTTCAA
m-Cxcl11-F	GGCTTCCTTATGTTCAAACAGGG
m-Cxcl11-R	GCCGTTACTCGGGTAAATTACA
m-Cxcl12-F	TGCATCAGTGACGGTAAACCA
m-Cxcl12-R	TTCTTCAGCCGTGCAACAATC
m-IL6-F	TAGTCCTTCCTACCCCAATTTCC
m-IL6-R	TTGGTCCTTAGCCACTCCTTC
m-IL10-F	TGAATTCCCTGGGTGAGAAGC
m-IL10-R	CACCTTGGTCTTGGAGCTTATT
For CUT&Tag	
Spike-in-Promoter-F	GCAGGAAAAGGAGGACGTGT
Spike-in-Promoter-R	TCGACGCTTTCTTGTTCGTA
CCL2-Promoter-F	TCATTTGCTCCCAGGAGTGG
CCL2-Promoter-R	GAGTAAGTGCAGAGCCCTCG
CXCL2-Promoter-F	CTGTGCTTCCTGATGAGGGG

CXCL2-Promoter-R	CCCGAGAGCTCCTTTTATGCA
CXCL3-Promoter-F	TGGGGCCCTATCTTCCTTCT
CXCL3-Promoter-R	GATGACTGGAAGAGCCCGAG
For shRNAs	
mHSP47-sh1-F	CCGGGACAAGAACAAGGCAGACCTACTCGAGTAGGTCTGCCTTGTTCTTGTCTTTTTG
mHSP47-sh1-R	AATTCAAAAAGACAAGAACAAGGCAGACCTACTCGAGTAGGTCTGCCTTGTTCTTGTC
mHSP47-sh2-F	CCGGCGAACACTCCAAGATCAACTTCTCGAGAAGTTGATCTTGGAGTGTTCGTTTTTG
mHSP47-sh2-R	AATTCAAAAACGAACACTCCAAGATCAACTTCTCGAGAAGTTGATCTTGGAGTGTTCG